geosciences

MDPI

Article

Composition Changes of Hydrocarbons during Secondary Petroleum Migration (Case Study in Cooper Basin, Australia)

Sara Borazjani, David Kulikowski, Khalid Amrouch and Pavel Bedrikovetsky *

Australian School of Petroleum, The University of Adelaide, Adelaide, South Australia 5005, Australia; sara.borazjani@adelaide.edu.au (S.B.); david.kulikowski@adelaide.edu.au (D.K.); khalid.amrouch@adelaide.edu.au (K.A.)

* Correspondence: pavel.bedrikovetski@adelaide.edu.au

Received: 28 November 2018; Accepted: 30 January 2019; Published: 3 February 2019

Abstract: The reliable mathematical modelling of secondary petroleum migration that incorporates structural geology and mature source rocks in the basin model, allows for prediction of the reservoir location, yielding the significant enhancement of the probability of exploration success. We investigate secondary petroleum migration with a significant composition difference between the source and oil pools. In our case study, the secondary migration period is significantly shorter than the time of the hydrocarbon pulse generation. Therefore, neither adsorption nor dispersion of components can explain the concentration difference between the source rock and the reservoir. For the first time, the present paper proposes deep bed filtration of hydrocarbons with component kinetics retention by the rock as a physics mechanism explaining compositional grading. Introduction of the component capture rate into mass balance transport equation facilitates matching the concentration difference for heavy hydrocarbons, and the tuned filtration coefficients vary in their common range. The obtained values of filtration coefficients monotonically increase with molecular weight and consequently affects the size of the oleic component, as predicted by the analytical model of deep bed filtration. The modelling shows a negligible effect of component dispersion on the compositional grading.

Keywords: secondary migration; sedimentary basin; composition gradient; stress-dependent permeability; deep-bed filtration; mathematical model

1. Introduction

Secondary migration of hydrocarbons is a buoyant flow from the source rock upward along the carrier bed, resulting in the formation of petroleum accumulation (Figure 1). Mathematical modelling of secondary petroleum migration facilitates restoration of the basin history and is important for oil and gas exploration, for identification of geologic traps as candidates for oil-gas reservoirs, and for planning the exploratory drilling [1].

Mathematical models for secondary migration of single-phase multicomponent oil-gas fluids reflect numerous processes of mass transfer between the rock and fluid occurring during secondary migration of hydrocarbons [2–9]. Regarding flow simulation during secondary petroleum migration, the models includes non-equilibrium adsorption and its hysteresis, diffusion and dispersion, and advective transport with Darcy's velocity [10–14]. The diffusive flux encompasses concentration-, thermal- and baro-diffusion [15–18].

The models describe depth variation of fluid composition with depth due to gravity. Under steady state of a single-phase multicomponent column and assuming constant temperature, the thermodynamic equilibrium corresponds to a constant total of chemical and gravity potentials [19,20]. This provides the

equations for component depth distribution, allowing for predicting compositional gradients in thick formations. The deviation between the modelling and field data is attributed to the effects of the Earth thermal gradient [21–23].

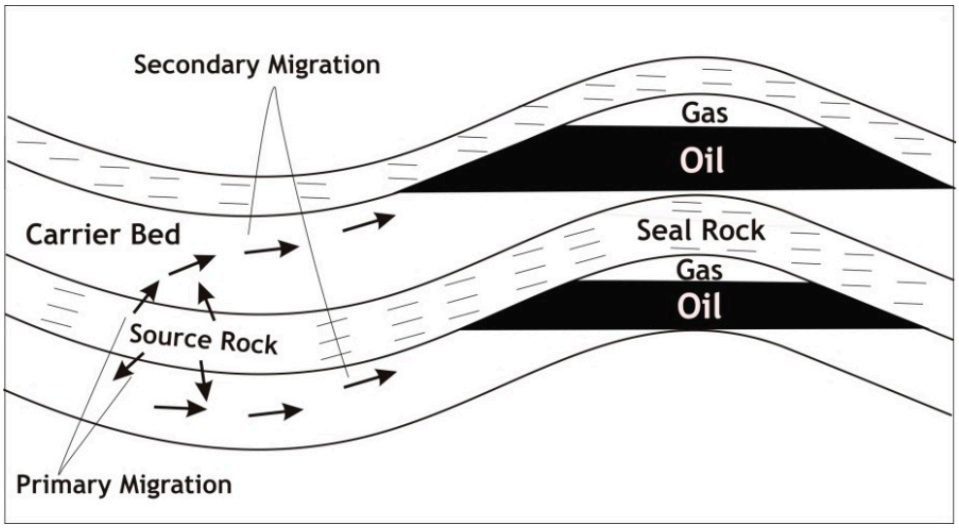

Figure 1. Secondary petroleum migration from source rock to stratigraphic trap.

The systems with temperature varying along space coordinates are not in the state of thermodynamic equilibrium [24]. Book [11] provides a detailed derivation of equations for depth distribution of components accounting for the Earth temperature gradient based on non-equilibrium thermodynamics. The depth concentration distribution corresponds to zero overall diffusive flux for each component, including thermos- and baro-diffusion. The model enables predicting the depth distribution of components due to gravity and the vertical thermal gradient [25,26].

Extensions of the thermo-gravitational equilibrium conditions for two- and three-phase multicomponent fluids with adsorption and chemical reactions are presented in works [21–23,27,28]. Being implemented into software Themis, the mathematical models for secondary migration predict compositional gradients of petroleum fluids due to losing their heavy components by adsorption during secondary migration [5–9].

Despite this, non-adsorption mechanisms of the petroleum component retention in rocks haven't been considered in the mathematical models.

In the present paper we discuss secondary migration in the Cooper-Eromanga Basin, where a significant difference between composition of oils in source rock and in the reservoir was noticed. The Cooper-Eromanga basin is Australia's largest onshore hydrocarbon province and lies across the border of South Australia and Queensland. Hydrocarbons are typically produced from Permian-Triassic (Cooper Basin) and Jurassic-Cretaceous (Eromanga Basin) fluvial reservoirs [29,30].

The aim of this study is to provide an explanation of the observed compositional gradients using mathematical modelling and matching the field data. In the case under investigation, the pulse generation period is significantly longer than the breakthrough (flight) time of components. We explain the difference between oil component concentrations in source rock and in the oil reservoir involving the non-adsorption mechanical retention of long hydrocarbon chains by the rock grains [31]. Hydrocarbons do adsorb on the initially water-saturated rock, yielding concentration decreases along the migrating oil. However, the adsorption stops after the component breakthrough during long periods of secondary migration and cannot cause the concentration difference between the source rock and the reservoir. The dispersivity length is significantly shorter than the migration path, so dispersion/diffusion cannot cause the concertation difference either [10,11,32]. Therefore, petroleum-migration transport phenomena other than adsorption and dispersion, explaining the concentration difference, must be identified.

The alternative mechanism for concentration grading for colloids in porous media is so called deep bed filtration. For polymer transport in porous media, adsorption has been considered to be the only capture process since late 1950 [10,11,33,34]. However, the laboratory data on polymer flow with continuous increase in pressure drop, which cannot be explained by polymer adsorption, have been reported recently for coreflooding and for well injectivity [31,35]. The concentration difference between injected polymers at the core inlet (injection well) and core effluent (polymer in the production well) was successfully explained by deep bed filtration (particulate transport with capture by the rock) of polymer molecules in porous media [31]. Different polymer capture mechanisms, like straining, attachment, diffusion into dead-end pore and stagnant zones, have been discussed. High levels of agreement between the laboratory-based prediction of well behaviour and that for field data were observed [35]. Adsorption and filtering of polymers and hydrocarbons in porous media are not mathematically equivalent [11,31,35,36]. However, deep bed filtration modelling for secondary migration of hydrocarbons for interpretation and analysis of the concentration gradients hasn't been developed.

In the present paper, for the first time we propose deep bed filtration of hydrocarbons in carrier beds to explain the difference between oil compositions in source rock and the reservoir by retention of hydrocarbon molecules in carrier bed. Consequently, we use the analytical model for 1D colloidal flow with capture of large oleic molecule the field data on oleic compositions in source rock and in the reservoir were successfully matched by tuning the filtration coefficient foe all components. The obtained filtration coefficient increases with the increase in number of carbon atoms in hydrocarbon molecules, as is expected from deep bed filtration theory [36–44]. However, this is not the case for light hydrocarbons, which is explained by their evaporation in the associated gas during the secondary migration. The sensitivity study shows that the effect of component diffusion / dispersion on the compositional grading due to component retention is negligible. We also show how a decrease of permeability with depth results in higher compositional gradients.

The structure of the paper is as follows. Section 2 formulates the problem of explaining the concentration gradients in the case of secondary petroleum migration, where the pulse liberation period is significantly larger than the flow time between the source rock and the stratigraphic trap. Section 3 presents basics of deep bed filtration in porous media. Section 4 derives the analytical model for migration with particle retention by the rock. Section 5 discusses the results of numerical data treatment by the analytical model. Section 6 presents a qualitative analysis of the rock stress effects in the carrier bed on the hydrocarbon filtering. Section 7 concludes the paper.

2. Formulation of the Problem and Study Methodology

In this section we formulate the problem of compositional grading between source rock and the reservoir and show how the phenomena will be explained using single phase multi-component transport phenomena in the carrier bed.

Figure 2 shows the ratio of source rock concentration to the reservoir concentrations (c/c_{res}) of hydrocarbons versus the number of carbon atoms in four wells of two different oil pools. The aim of this work is to explain the difference in oil compositions.

Figure 3a shows the basement fault map of the study area and the location of the four wells used in this study [45–48]. Hydrocarbon compositions were obtained from the Permian Patchawarra Formation source rock at G27 and G42 [24,49]. The migrated oil compositions were obtained from Jurassic reservoirs in G27 and G42, which migrated through fault conduits and also from Tantanna 2 and Sturt East 1, where oil has migrated through a permeable carrier bed from the Gidgealpa location (Figure 3b). The Permian outer edge illustrates the location where the Triassic seal pinches out and enables the Permian source rock to lie directly below Jurassic reservoirs, and this is reflected by the large number of producing oil pools in that location.

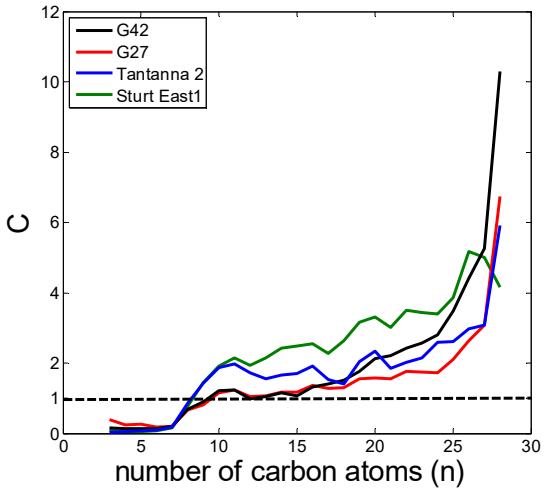

Figure 2. The ratio between concentration of hydrocarbons in source rock and in the reservoir in four wells.

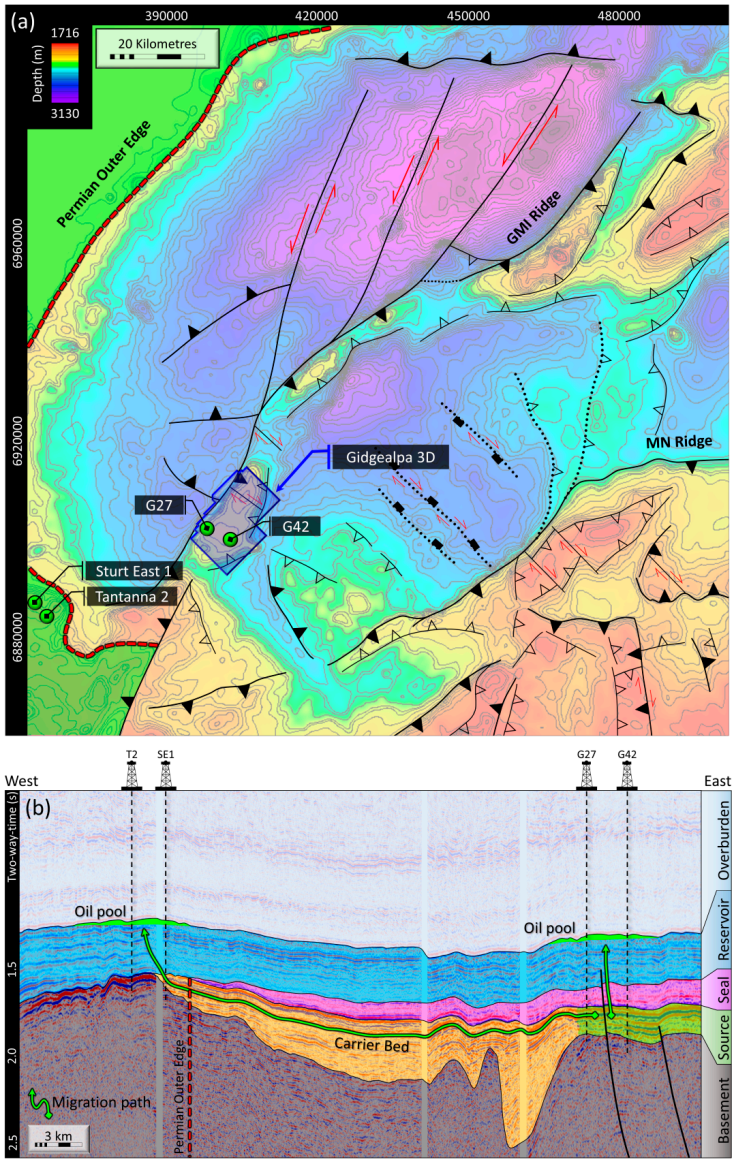

Figure 3. Structural interpretation of the Cooper-Eromanga Basin showing the location of wells, the Permian outer edge (where Triassic seal pinches out), and the migration of oil from source rocks to

traps: (**a**)—Basement fault map of the study area showing the location of the four wells used in this study. Source rock composition was obtained from the Patchawarra Formation in wells G27 and G45. The expelled oil migrated along two pathways, vertically through large basement faults and laterally through a carrier bed. The oil compositions in the Jurassic reservoir are obtained from G27 and G45 wells (vertical migration through faults), and Tantanna 2 (T1) and Sturt East 1 (SE1) (lateral migration through carrier bed). [24,49]; (**b**) showing the two migration paths from the source rock in the Gidgealpa region to the oil pools through faults and via sedimentary rocks. The Permian outer edge shows the location where Triassic seals pinch-out, allowing oil to freely migrate from the source rock to the overlying reservoir rock.

Figure 4a illustrates the timing to hydrocarbon expulsion in the Cooper Basin. Initial generation commenced in the Late Permian and peaked during the Mid-Cretaceous, with present-day generation potential existing in favourable portions of the basin given sufficiently high temperatures and the presence of residual kerogen [50]. Figure 4b illustrates the key petroleum system events for the Cooper-Eromanga petroleum system. The Permian Patchawarra Formation source rocks reached initial thermal maturity in the Late Permian, with hydrocarbon generation and migration continuing today. Given the ~260 million-year generation window, the duration of hydrocarbon migration from source to the Jurassic reservoir is short. Therefore, the migration of components is considered to be steady-state. As such, the adsorbed concentration in each point of the migration path is already established up to the value that is in equilibrium with concentrations in the solute. Therefore, adsorption does not change concentrations of hydrocarbons along the migration path. The concentration profiles become steady-state after the component breakthrough.

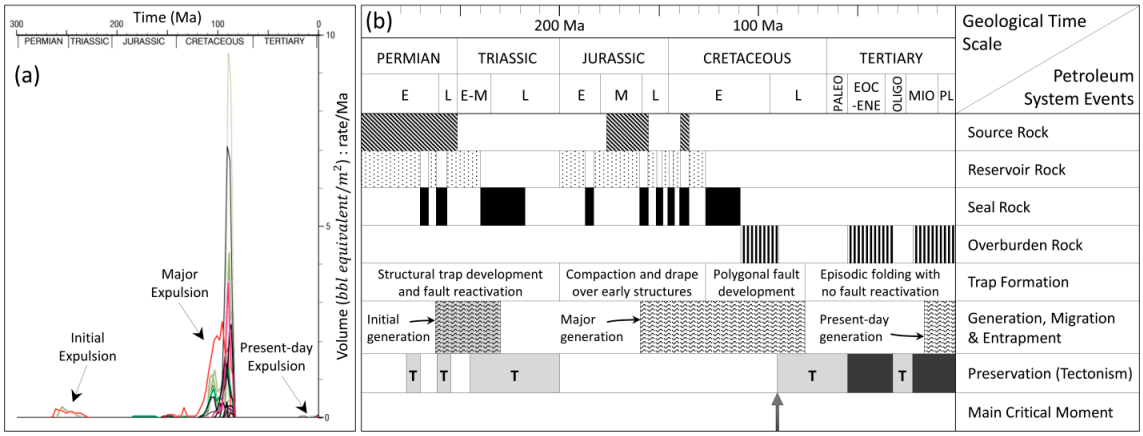

Figure 4. Summary of the Cooper-Eromanga Petroleum System Events: (**a**)—The timing of hydrocarbon generation and expulsion through time showing that initial expulsion commenced in the Late Permian and continues today [50]; (**b**) A summary of the key petroleum system events in the Cooper-Eromanga Petroleum System [30].

Dispersion/diffusion at the large length scale of the carrier bed is negligible if compared with the advective flux, and also does not contribute to the component variation.

The next section considers and explains an ultimate mechanism for compositional grading in the kinetic component by the rock, known as deep bed filtration. Here we consider non-steady-state component capture by the rock as a source for non-uniform component concentration profiles.

3. Deep Bed Filtration of Colloidal Suspensions in Porous Media

In this section we consider physics for size exclusion of large oleic molecule. During flow in natural and artificial rocks, fine particles are captured by the skeleton [36–39]. The schematic for deep bed filtration is presented in Figure 5. The figure shows particle retention by straining, attachment and

mechanical entrapment. For straining and size exclusion, we consider the jamming ratio, which is the ratio between the particle size r_s and pore size r_p

$$j = \frac{r_s}{r_p} \tag{1}$$

Here for large hydrocarbon molecule with $n = 20$, $r_s = 27 \times 10^{-10}$ m. Average pore size can be estimated from permeability and porosity

$$r_p = 5\sqrt{\frac{k}{\phi}} \tag{2}$$

Porosity and permeability in the carrier bed are 0.105 and 1mD, respectively. As such, the jamming ratio for hydrocarbon $n = 20$ is 0.0018. Usually, size exclusion corresponds to $j > 0.1$ [39–41]. For lower jamming ratios, straining in thin pores, micro-cracks and crevices may occur.

The total retention rate is proportional to particle advective flux. The proportionality coefficient is called the filtration coefficient (λ). The filtration coefficient is a ratio between the capture probability and the rock dispersivity, i.e., it is equal to capture probability per unit length of the migration trajectory [36]:

$$\frac{\partial \sigma_n}{\partial t} = -\lambda_n c_n U, \quad \lambda_n = \frac{p_n}{l} \tag{3}$$

The filtration coefficient is equal to reciprocal of the retention-free distance of the particle transport [36,38,42]. Usually, the filtration coefficient varies from 0.001 to 10 1/m for low-retention transport of colloids up to 100–1000 1/m for injection of high-concentration suspensions [4,36,43].

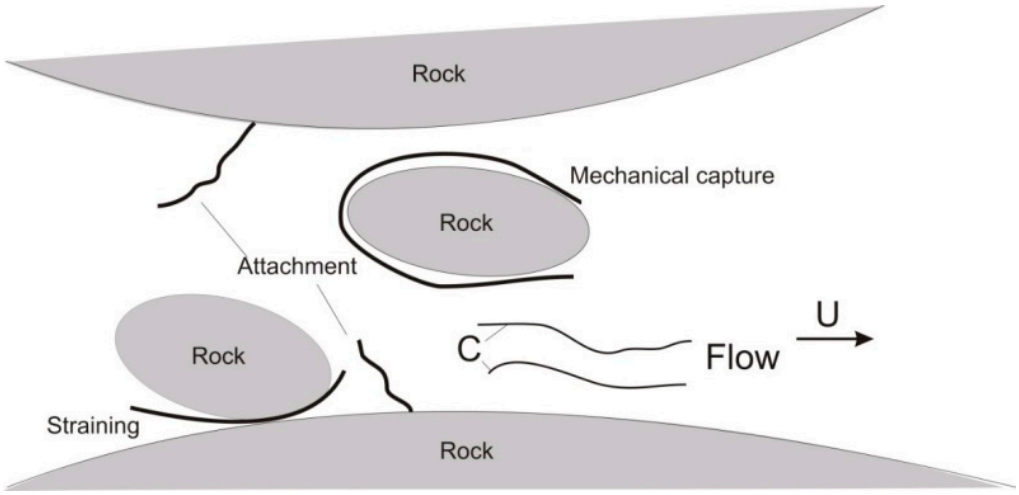

Figure 5. Schematic of deep bed filtration in porous media. Particle retention by straining, attachment and mechanical entrapment. *C* presents the hydrocarbon component and *U* is the flow velocity.

4. Mathematical Model for Secondary Migration with Particle Retention

The physical schematic of deep bed filtration presented in this section presents the assumptions of the mathematical model (Section 4.1), analytical solution (Section 4.2) and matching the field data (Section 4.3).

4.1. Assumptions of the Model

The time of pulse generation from the Patchawarra Formation source rocks began in the Late Permian and continues today (~260 million years), while the migration of expelled oils to Jurassic reservoirs was relatively fast given the short pathway distances of <1 km (fault migration) and ~40 km

(carrier bed pathway) (Figures 3 and 4) [49,51]. Given the high ratio between the pulse duration and migration time, the secondary migration flow of each component is considered to be steady state.

We assume one dimensional steady state multicomponent flow from source rock to oil reservoir, formation brine and migrating oil to be uncompressible, where oleic components diffuse with respect to mean velocity. The components are adsorbed and captured by the rock due to attachment, straining, or bridging. The model assumes that each component can be captured by the rock. The capture mechanisms include diffusion into dead-end pores and pore-scale gravity segregation, so even light components can be subject to a capture. However, for the steady state component transport we assume that adsorbed concentrations have already been reached during the transient secondary migration after the breakthrough time. Therefore, component adsorption is not present in the steady-state flow model.

4.2. Analytical Model for Steady-State Flow of Components

Consider one dimensional advective-diffusive flow with capture of each component by the rock [10,32,36,37]:

$$U\frac{\partial c_n}{\partial x} = \alpha_L U\frac{\partial^2 c_n}{\partial x^2} - \lambda_n c_n U \tag{4}$$

where c_n is the concentration of n-th component in the migrating fluid, U is the flux velocity, α_L is the dispersivity and λ is the filtration coefficient.

Introducing the following dimensionless parameters

$$X = \frac{x}{L}; C_n = \frac{c_n}{c_{n_{res}}}; \Lambda_n = \lambda_n L \tag{5}$$

We obtain the following flow equation

$$\frac{\partial C_n}{\partial X} = \frac{\alpha_L}{L}\frac{\partial^2 C_n}{\partial X^2} - \Lambda_n C_n \tag{6}$$

The boundary condition at $X = 0$ correspond to oil composition liberated by source rock into the carrier bed:

$$X = 0: \quad C_n = C_{n_I} \tag{7}$$

The boundary condition at $X = 1$ correspond to no-diffusion at the impermeable outlet [52]

$$X = 1: \quad \frac{\partial C_{n_I}}{\partial X} = 0 \tag{8}$$

According to dimensionalisation given by Equation (5),

$$X = 1: \quad C_n = 1 \tag{9}$$

Second order linear ordinary differential equation (ODE) always has a real decrement, because α_L/L is positive [53].

The solution of ODE (6) is

$$C_n = Ae^{\frac{1-\sqrt{1+4\frac{\alpha_L}{L}\Lambda_n}}{\frac{2\alpha_L}{L}}X} + Be^{\frac{1+\sqrt{1+4\frac{\alpha_L}{L}\Lambda_n}}{\frac{2\alpha_L}{L}}X} \tag{10}$$

Boundary conditions (7)–(9) define constants A, B and Λ.

The solution of the problem in (10) is shown in Figure 6 for n = 11, 13 and 14.

For slow flow in heterogeneous reservoirs we consider the dispersivity ration α_L/L varies between 10^{-3} and 10^{-1} [10,11]. Therefore, diffusion can be neglected, and solution (10) degenerates into the solution of the following system

$$\frac{dC_n}{dX} = -\Lambda_n C_n \tag{11}$$

$$\begin{array}{l} X = 0: \quad C_n = C_{n_I} \\ X = 1: \quad C_n = 1 \end{array} \tag{12}$$

4.3. Determination of Filtration Coefficient Versus X

The solution of ordinary differential Equation (11) with boundary condition (12) is [37,39]

$$C_n = C_{n_I} e^{-\Lambda_n X} \tag{13}$$

The profiles of concentration are shown in Figure 6 for n = 11, 13, 14. The difference between profiles with and without diffusion is negligible if compared with the values of concentrations.

We consider concentrations in the reservoir to be known. This allows for determining the filtration coefficient using Equation (13).

$$\Lambda_n = \ln\left(C_{n_I}\right) \tag{14}$$

The numerical treatment of the field data using Equations (13) and (14) will be presented in the next section.

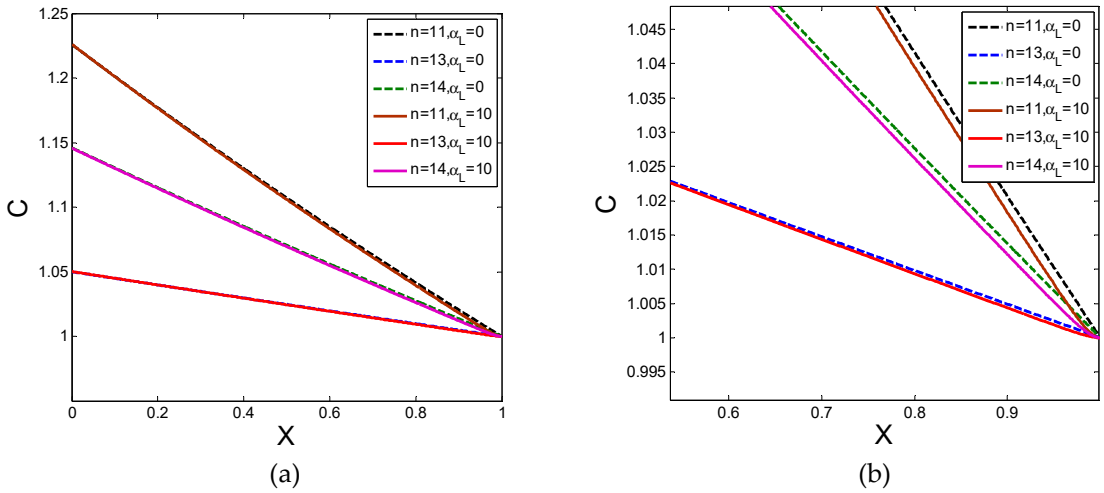

Figure 6. Concentration profiles of hydrocarbons for n = 11, 13, and 14 for path through the fault in G42: (**a**) profiles throughout the fault; (**b**) zoom near to production wells in the reservoir. Solid lines—flow with diffusion; dashed lines—diffusion-free flow.

5. Numerical Results

The numerical solutions of Equation (14) subject to boundary condition (12) are presented in Figure 7. For $n > 10$ the higher the carbon numbers, the higher the filtration coefficient. This corresponds to larger molecular weight and higher electrostatic attraction to the rock [54]. Also, long chains of molecule with high carbon numbers are easily strained between grains. However, for light and intermediate hydrocarbon $n < 10$ the trend is in the opposite direction, where the higher the carbon number the lower the filtration coefficient, which is explained by evaporation of a large component into a gas phase. The lighter components evaporate more intensively, which causes a decrease of their concentration in the oleic phase and effectively decreases the filtration coefficient as calculated by Equation (14).

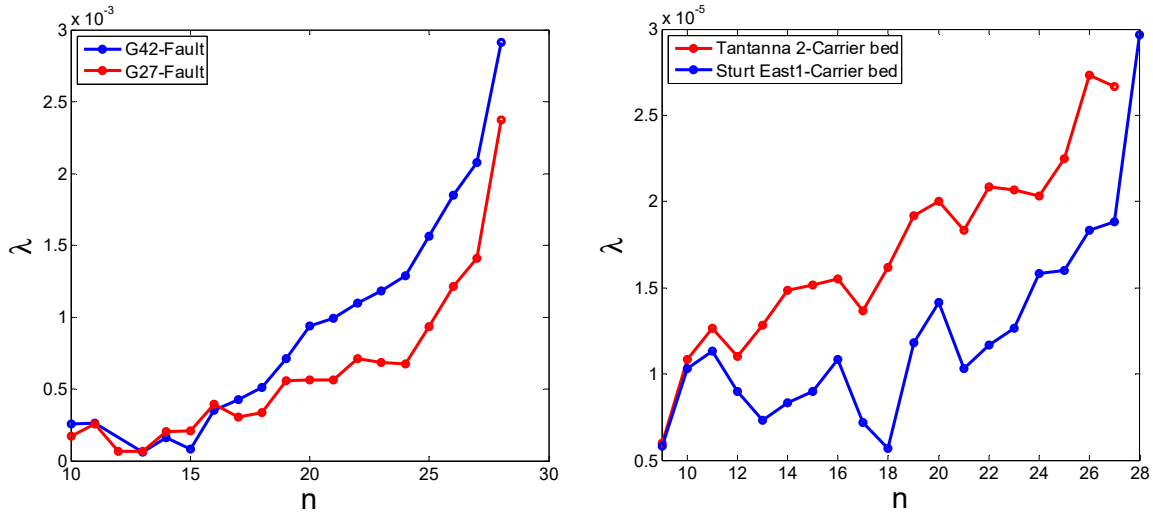

Figure 7. Filtration coefficients for hydrocarbons with difference carbon numbers for four different flow paths: (**a**) for wells G42 and G27, (**b**) for wells T2 and SE1.

Column 2–9 in the Table 1 corresponds to dimensional filtration coefficients the values of filtration coefficient have order of magnitude of those for multi-component fluxes in porous media.

For conditions of secondary migration, time of secondary migration is 2-3 orders of magnitude lower than the production pulse period.

Because the jamming ratio for large hydrocarbon molecules is significantly smaller than one, size exclusion is unlikely. However, DLVO attraction with consequent attachment and diffusion in dead-end pores is feasible.

The permeability of open faults is significantly higher than in sedimentary rocks. As such, pore sizes in open faults are also significantly higher than in sedimentary rocks. For the same long hydrocarbon macro-molecules, the jamming ratio in sedimentary rocks is lower than that in the faults. The electrostatic attraction in wider pores and micro channels is lower. The above-mentioned factors determine that filtration coefficients in sedimentary rocks are significantly lower than in open faults. Indeed, the 2–4 columns in Table 1 and Fig. 6a exhibit significantly lower filtration coefficients in rocks than in faults (column 5–7 in Table, Figure 6b).

The adsorption coefficients for hydrocarbons on sandstones is well known [34]. Deep bed filtration coefficients for hydrocarbons are determined in the paper for the first time. The obtained values of filtration coefficient allow the prediction of component concentrations in other geological traps.

Upscaling of the micro-scale equations up to the carrier bed scale shows that the dispersivity depends on scale [10]. Capture probability also depends on the scale [36]. The values of filtration coefficients have been obtained from the field data, i.e. for the reservoir scale. Therefore, unsteady state solution $c(x,t)$ with filtration coefficients determined in the present paper (Table 1) can serve for prediction of hydrocarbon concentrations in the reservoir after short-time pulse generation.

Table 1. Results of concentration data treatment for four wells.

Carbon Number n	$\lambda \times 10^3$ 1/m, without Diffusion, for Well G42	$\lambda \times 10^3$ 1/m, with Diffusion, for Well G42, α_L = 10 m	$\lambda \times 10^3$ 1/m, without Diffusion, for Well G27	$\lambda \times 10^3$ 1/m, with Diffusion, for Well G27, α_L = 10 m	$\lambda \times 10^4$ 1/m, without Diffusion, for Well T2	$\lambda \times 10^4$ with Diffusion for Well T2 α_L = 100	$\lambda \times 10^4$ 1/m, without Diffusion, for SE1	$\lambda \times 10^4$ with Diffusion for Well SE1 α_L = 100
2	0.314	0.319			0.25	0.25		
9					0.06	0.06	0.058	0.058
10	0.255	0.265	0.173	0.176	0.108	0.108	0.103	0.103
11	0.261	0.259	0.259	0.2635	0.127	0.127	0.113	0.113
12			0.066	0.067	0.11	0.11	0.09	0.09
13	0.0615	0.0617	0.0853	0.0866	0.128	0.128	0.073	0.073
14	0.170	0.173	0.2024	0.205	0.148	0.148	0.083	0.083
15	0.083	0.082	0.206	0.209	0.152	0.152	0.09	0.09
16	0.3541	0.358	0.393	0.400	0.155	0.155	0.108	0.108
17	0.429	0.434	0.304	0.309	0.137	0.137	0.072	0.072
18	0.5215	0.529	0.337	0.342	0.162	0.162	0.056	0.056
19	0.715	0.726	0.558	0.567	0.192	0.192	0.118	0.118
20	0.941	0.961	0.568	0.576	0.2	0.2	0.142	0.142
21	0.994	1.01	0.558	0.567	0.183	0.183	0.103	0.103
22	1.11	1.13	0.712	0.721	0.208	0.208	0.117	0.117
23	1.18	1.21	0.690	0.7	0.207	0.207	0.126	0.126
24	1.288	1.32	0.68	0.69	0.203	0.203	0.158	0.158
25	1.56	1.60	0.931	0.956	0.225	0.225	0.16	0.16
26	1.85	1.90	1.22	1.241	0.273	0.273	0.183	0.183
27	2.07	2.15	1.41	1.45	0.267	0.267	0.188	0.188
28	2.91	3.04	2.38	2.46	0.233	0.233	0.296	0.296

6. Effects of Stress on Compositional Gradients of Migrating Oil

The above sections describe buoyant secondary migration with deep bed filtration. This flow is accompanied by decreasing of depth along the trajectory, which results in a decrease of stress; this effect is not accounted in the above calculations. In this section, we account for varying stress with consequent change in oil filtrating by the carrier bed with depth. Deep bed filtration of oil through carrier beds is accompanied by the capture of the high-molecular-weight oleic components by thin pore throats, crevices between grains, and micro-cracks. The capture mechanisms are size exclusion and straining, i.e. the mechanical retention of large molecules occurs. The permeability and porosity may significantly change along the migration path due to pore stress/pore pressure variation with depth and along the path. Rock deformation under high pressure can cause a significant reduction of pore throat size and pore collapse, yielding an increase of the capture probability, and, consequently enhancing the component concentration gradients between the source rock and reservoir oils. Below we show some relationships between the filtration coefficient and depth. Being applied along the carrier bed, these relationships can account for the stress effects on deep bed filtration of the migrating oil. The resulting equations do not allow for simple solutions, so the corresponding numerical reservoir modelling is a topic of a separate work. However, the qualitative effects can be drawn directly.

Vertical force balance exerting the column with thickness H is [55]

$$\rho g H = \sigma_v + \alpha p_{res} \tag{15}$$

where ρ is the density of rock saturated by water, g is the gravity, p_{res} is a pore (reservoir) pressure, σ_v is the vertical component of stress, and α is the Biot's coefficient.

The reservoir pressure assuming connection of the reservoir to an aquifer is equal to the hydrostatic pressure [56]

$$\rho_w g H = p_{res} \tag{16}$$

Rock permeability and porosity are given by stress compressibility dependencies for deformable rocks

$$k = k\left(\sigma_{eff}\right), \quad \phi = \phi\left(\sigma_{eff}\right) \tag{17}$$

Substituting Equation (15) into Equation (16), we obtain the following formula for the vertical stress component:

$$\sigma_v = gH((1-\phi)\rho_r + (\phi - \alpha)\rho_w) \tag{18}$$

Example

For typical values of porosity and rock and density values, the right hand side of Equation (18) is positive. For example, for ϕ = 0.3, α = 0.8, ρ_w = 1 g/cm^3, ρ_r = 2.6 g/cm^3, the coefficient in the bracket at gH right hand side of Equation (18) is equal to 1.32. Therefore, the vertical stress increases with depth. For usual depth variations of lateral stress, the effective stress σ_{eff} also increases with depth (see Equation (15)). Consider two reservoirs with 1km (reservoir a) and 10 km (reservoir b) depth. Equation (16) defines the reservoir pressures, p_{resa} = 1 and p_{resb} = 10 MPa respectively. Using Equation (18) vertical stresses are equal to 17MPa and 170 MPa, respectively. According to monotonically decreasing relationships (17), permeability and porosity also decrease with depth. However, the relative decrease of permeability is significantly higher than that of porosity, so the average pore throat radius, according to Equation (2), decreases with depth. Finally, the pore radius decreases with depth, so the filtration coefficient due to size exclusion increases, yielding the increase in compositional gradients in migrating oil along the pathway.

7. Discussions

Adsorption of component decreases its concentration in the flux. Adsorption can explain the concentration difference between the source and the reservoir for short-term pulses, since different

components adsorb on the rock differently. However, in our case, the generated pulse duration highly exceeds the migration time, so adsorption does not occur after the component breakthrough.

Diffusion promotes a mixture zone, so the breakthrough time for different components is different, which could cause a compositional grading. Yet, for large geological scales, the component diffusion and dispersion can be neglected if compared with the advective buoyant flux.

We propose mechanical or electrostatic capture of long hydrocarbon molecules by rock grains as a physics mechanism to explain the compositional grading. The petroleum fluids are represented as colloidal suspensions of long hydrocarbon molecules, which can be captured by the rock during secondary migration. The introduction of particle deep-bed-filtration term in the governing system, allows matching of the concentrations in the source and in the reservoir. The obtained filtration coefficients for heavy hydrocarbons have the same order of magnitude as those obtained in suspension-colloidal flow in porous media. It allows assuming steady-state suspended concentration distribution during secondary migration occurs with the capture of heavy hydrocarbon components.

Yet, only two compositions, in the source rock and in the reservoir, are available. The only information for the model coefficients that can be extracted from those data is the filtration coefficient. For the cases where the residual oil composition along the migration path is known, more detailed matching by the mathematical model can be achieved.

The filtration coefficients as obtained from oil compositions in source rock and in the reservoir, are monotonically increasing as carbon number increases. The monotonicity takes place at heavy hydrocarbons, for $n > 10$. Loss of monotonicity for light and intermediate hydrocarbons can be explained by their evaporation into gas phase.

The explanation of light and intermediate hydrocarbons into the gas phase is supported by their concentrations in oil, which are higher in source rock than in the trapped reservoir oil.

Incorporating rock compressibility, stress variation and two-phase oil-gas buoyant flow in the governing equations would make the data of mathematical modelling significantly more reliable. It would allow for predictive modelling for significantly wider class of petroleum basins. However, the model (4) used explains the compositional grading in the investigated flow pattern of the Cooper-Eromanga basin.

8. Conclusions

Through analysis of the field data on oil compositional gradients using the analytical model for capture of hydrocarbons by the rock during secondary migration, the following can be concluded:

- An analytical model for deep bed filtration of petroleum components facilitates matching the component concentrations in source rock and reservoir.
- For heavy hydrocarbons with n>10, the obtained values of filtration coefficients vary in the typical intervals. The heavier the component, the larger the filtration coefficient.
- For light and intermediate hydrocarbons with n<10, the tendency of monotonicity does not take place, which is explained by evaporation into associated gas phase that migrates together with oil.
- Comparison between modelling with and without the component dispersion shows a negligible effect of dispersion on compositional difference between the source rock and petroleum reservoir.
- Higher stress yields to the lower porosity and lower permeability, which results in a smaller pore size and higher deep bed coefficients.

Author Contributions: Writing—original draft, S.B. and P.B.; Writing—review & editing, D.K. and K.A.

Funding: This research received no external funding.

Conflicts of Interest: The authors declare no conflict of interest.

References

1. England, W.A.; Mann, A.L.; Mann, D.M. *Migration from Source to Trap: Chapter 3: Petroleum Generation and Migration*; BP Research: London, UK, 1991.
2. Magoon, L.B.; Dow, W.G. The petroleum system-from source to trap. *AAPG Mem.* **1994**, *60*, 1–24.
3. Siddiqui, F.I.; Lake, L.W. A dynamic theory of hydrocarbon migration. *Math. Geol.* **1992**, *24*, 305–327. [CrossRef]
4. Helset, H.M.; Lake, L.W. Three-phase secondary migration of hydrocarbon. *Math. Geol.* **1998**, *30*, 637–660. [CrossRef]
5. Bessis, B.; Burrus, F.; Ungerer, J.P.; Chenet, P.Y. Integrated Numerical Simulation of the Sedimentation Heat Transfer, Hydrocarbon Formation and Fluid Migration in a Sedimentarybasin, the THEMIS Model. In *Thermal Modelling in Sedimentary Basins*; Burrus, J., Ed.; Technip: Paris, France, 1986; pp. 173–195.
6. Galushkin, Y. Non-Standard Problems in Basin Modelling. Springer International Publishing: Basel, Switzerland, 2016.
7. Baur, F.; Scheirer, A.H.; Peters, K. Past, present and the future of basin and petroleum system modeling. *AAPG Bull.* **2017**, *102*, 549–561. [CrossRef]
8. Peters, K.E.; Schenk, O.; Scheirer, A.H.; Wygrala, B.; Hantschel, T. Basin and Petroleum System Modeling. In *Springer Handbook of Petroleum Technology 2017*; Springer: Cham, Switzerland, 2017; pp. 381–417.
9. Baur, F.; Katz, B. Some practical guidance for petroleum migration modelling. *Mar. Pet. Geol.* **2018**, *93*, 409–421. [CrossRef]
10. Lake, L.W. *Enhanced Oil Recovery*; Prentice Hall: Englewood Clis, NJ, USA, 1989.
11. Bedrikovetsky, P.G. *Mathematical Theory of Oil & Gas Recovery*; Kluwer Academic Publishers: London, UK; Boston, MA, USA; Dordrecht, The Netherlands, 1993.
12. Carruthers, D. Modeling of Secondary Petroleum Migration Using Invasion Percolation Techniques. In *AAPG/Datapages Discovery Series: Multidimensional Basin Modeling*; Duppenbecker, S., Marzi, R., Eds.; AAPG/Datapages: Tulsa, OK, USA, 2003; pp. 21–37.
13. Carruthers, D.; Ringrose, P. Secondary oil migration: Oil-rock contact volumes, flow behaviour and rates. *Geol. Soc. Lond. Spec. Publ.* **1998**, *144*, 205–220. [CrossRef]
14. Carruthers, D.J.; de Lind van Wijngaarden, M. Modelling viscous-dominated fluid transport using modified invasion percolation techniques. *J. Geochem. Explor.* **2000**, *69–70*, 669–672. [CrossRef]
15. Dejam, M.; Hassanzadeh, H.; Chen, Z. A reduced-order model for chemical species transport in a tube with a constant wall concentration. *Can. J. Chem. Eng.* **2018**, *96*, 307–316. [CrossRef]
16. Dejam, M.; Hassanzadeh, H.; Chen, Z. Shear dispersion in a capillary tube with a porous wall. *J. Contam. Hydrol.* **2016**, *185–186*, 87–104. [CrossRef]
17. Dejam, M.; Hassanzadeh, H.; Chen, Z. Shear dispersion in a fracture with porous walls. *Adv. Water Resour.* **2014**, *74*, 14–25. [CrossRef]
18. Sun, Z.; Shi, J.; Wu, K.; Xu, B.; Zhang, T.; Chang, Y.; Li, X. Transport capacity of gas confined in nanoporous ultra-tight gas reservoirs with real gas effect and water storage mechanisms coupling. *Int. J. Heat Mass Transf.* **2018**, *126*, 1007–1018. [CrossRef]
19. Riemens, W.G.; Schulte, A.M.; De Jong, L.N.J. Bibra Field PVT variations along the hydrocarbon column and confirmatory field Test. *J. Petrol. Tech.* **1988**, *40*, 83–89. [CrossRef]
20. Wheaton, R.J. Treatment of variations of composition with depth in gas-condensate reservoirs. *SPE Reserv. Eng.* **1991**, *6*, 239–244. [CrossRef]
21. Shapiro, A.A.; Stenby, E.H. Two-Phase Segregation in a Thick Reservoir. In Proceedings of the ECMOR V-5th European Conference on the Mathematics of Oil Recovery, Leoben, Austria, 3–6 September 1996.
22. Montel, F.; Bickert, J.; Lagisquet, A.; Galliéro, G. Initial state of petroleum reservoirs: A comprehensive approach. *J. Pet. Sci. Eng.* **2007**, *58*, 391–402. [CrossRef]
23. Faissat, B.; Knudsen, K.; Stenby, E.H.; Montel, E. Fundamental statements about thermal diffusion for a multicomponent mixture in a porous medium. *Fluid Ph. Equilib.* **1994**, *100*, 209–222. [CrossRef]
24. Kulikowski, D.; Amrouch, K. Combining geophysical data and calcite twin stress inversion to refine the tectonic history of subsurface and offshore provinces: A case study on the Cooper-Eromanga Basin, Australia. *Tectonics* **2017**, *36*, 515–541. [CrossRef]
25. Firoozabadi, A. *Thermodynamics of Hydrocarbon Reservoirs*; McGraw-Hill: New York, NY, USA, 1999; 353p.

26. Whitson, C.H.; Brulé, M.R. *Phase Behavior*; Henry, L., Ed.; Doherty Memorial Fund of AIME Society of Petroleum Engineers: Richardson, TX, USA, 2000.
27. Nikpoor, M.H.; Dejam, M.; Chen, Z.; Clarke, M. Chemical-gravity-thermal diffusion equilibrium in two-phase non-isothermal petroleum reservoirs. *Energy Fuels* **2016**, *30*, 2021–2034. [CrossRef]
28. Shapiro, A.A.; Stenby, E.H. On the nonequilibrium segregation state of a two-phase mixture in a porous column. *Transp. Porous Media* **1996**, *23*, 83–106. [CrossRef]
29. Heath, R.; McIntyre, S.; Gibbins, N. A Permian Origin for Jurassic Reservoired Oil in the Eromanga Basin. In *The Cooper and Eromanga Basins, Australia*; O'Neil, B.J., PESA, SPE, SEG, Eds.; Petroleum Society of Australia: Adelaide, Australia, 1989; pp. 405–415.
30. Lowe-Young, B.S.; Mackie, S.L.; Heath, R.S. The Cooper-Eromanga petroleum system, Australia: Investigation of essential elements and processes. In Proceedings of the Petroleum Systems of SE Asia and Australasia Conference, Jakarta, Indonesia, 21–23 May 1997; pp. 199–211.
31. Farajzadeh, R.; Bedrikovetsky, P.; Lotfallahi, M.; Lake, L. Simultaneous sorption and mechanical entrapment during polymer flow through porous media. *J. Water Resour. Res.* **2016**, *52*, 2279–2298. [CrossRef]
32. Barenblatt, G.I.; Entov, V.M.; Ryzhyk, V.M. *Theory of Fluid Flows Through Natural Rocks*; Kluwer Academic Publishers: Dordrecht, The Netherlands, 1990.
33. Pope, G.A. The application of fractional flow theory to enhanced oil recovery. *SPE J.* **1980**, *20*, 191–205. [CrossRef]
34. Sorbie, K.S. *Polymer-Improved Oil Recovery*; Springer Science and Business Media: Berlin, Germany, 2013.
35. Lotfollahi, M.; Farajzadeh, R.; Delshad, M.; Al-Abri, A.-K.; Wassing, B.M.; Al-Mjeni, R.; Awan, K.; Bedrikovetsky, P. Mechanistic Simulation of Polymer Injectivity in Field Tests. *SPE J.* **2016**, *21*, 1–14. [CrossRef]
36. Bedrikovetsky, P. Upscaling of stochastic micro model for suspension transport in porous media. *J. Transp. Porous Media* **2008**, *75*, 335–369. [CrossRef]
37. Herzig, J.P.; Leclerc, D.M.; Le Goff, P. Flow of suspensions through porous media—Application to deep filtration. *J. Ind. Eng. Chem.* **1970**, *65*, 8–35. [CrossRef]
38. Bedrikovetsky, P.; You, Z.; Badalyan, A.; Osipov, Y.; Kuzmina, L. Analytical model for straining-dominant large-retention depth filtration. *Chem. Eng. J.* **2017**, *330*, 1148–1159. [CrossRef]
39. Bradford, S.A.; Simunek, J.; Bettahar, M.; Van Genuchten, M.T.; Yates, S.R. Modeling colloid attachment, straining, and exclusion in saturated porous media. *Environ. Sci. Technol.* **2003**, *37*, 2242–2250. [CrossRef] [PubMed]
40. Bradford, S.A.; Torkzaban, S. Colloid Transport and Retention in Unsaturated Porous Media: A Review of Interface-, Collector-, and Pore-Scale Processes and Models. *Vadose Zone J.* **2008**, *7*, 667–681. [CrossRef]
41. Elimelech, M. Particle deposition onideal collectors from dilute flowing suspensions: Mathematical formulation, numerical solution, and simulations. *J. Sep. Technol.* **1994**, *4*, 186–212. [CrossRef]
42. Elimelech, M.; Gregory, J.; Jia, X. *Particle Deposition and Aggregation*; Butterworth-Heinemann: Oxford, UK, 1995.
43. Pang, S.; Sharma, M.M. A Model for Predicting Injectivity Decline in Water-Injection Wells. *SPE J.* **1997**, *12*, 194–201.
44. Wennberg, K.E.; Sharma, M.M. Paper SPE 38181: Determination of the Filtration Coefficient and the Transition Time for Water Injection Wells. In Proceedings of the SPE European Formation Damage Conference, The Hague, The Netherlands, 2–3 June 1997.
45. Santos Ltd. *Gidgealpa 27 Well Completion Report; PPL 6 Moomba Block; Cooper & Eromanga Basins*; Santos Ltd.: Adelaide, Australia, 1988.
46. Santos Ltd. *Sturt East 1 Well Completion Report; PEL 5 and 6 Lake Hope Block; Cooper & Eromanga Basins*; Santos Ltd.: Adelaide, Australia, 1989.
47. Santos Ltd. *Tantanna 2 Well Completion Report; PEL 5 & 6 Lake Hope Block; Eromanga Basin*; Santos Ltd.: Adelaide, Australia, 1989.
48. Santos Ltd. *Gidgealpa 42 Well Completion Report; PPL 6 Moomba Block; Cooper & Eromanga Basins*; Santos Ltd.: Adelaide, Australia, 1991.
49. Kulikowski, D.; Amrouch, K.; Cooke, D.; Gray, M.E. Basement structural architecture and hydrocarbon conduit potential of polygonal faults in the Cooper-Eromanga Basin, Australia. *Geophys. Prospect.* **2017**. [CrossRef]

50. Deighton, I.; Hill, A.J. Thermal and burial history. In *Petroleum Geology of South Australia*; Gravestock, D.I., Hibburt, J., Drexel, J.F., Eds.; Petroleum Group: Adelaide, Australia, 1998; Volume 4, pp. 143–155.
51. Person, M.; Raffensperger, J.P.; Garven, G. Basin-scale hydrogeological modelling. *Rev. Geophys.* **1996**, *34*, 61–87. [CrossRef]
52. Logan, D.J. *Transport Modeling in Hydrogeochemical Systems*; Springer: New York, NY, USA, 2001.
53. Polyanin, A.; Zaitsev, V. *Handbook of Nonlinear Partial Differential Equations*; Chapman and Hall/CRC Press: Boca Raton, FL, USA, 2011.
54. Israelachvili, J. *Intermolecular and Surface Forces*; Academic Press: Millbrae, CA, USA, 2006.
55. Nicolaevskij, V.N. *Mechanics of Fractured and Porous Media. In World Scientific Series Theoretical and Applied Mechanics*; World Scientific: Singapore; Hackensack, NJ, USA; London, UK, 1990; Volume 8.
56. Dake, L.P. *The Practice of Reservoir Engineering*; Elsevier: Amsterdam, The Netherlands, 2013; Volume 36.